Dynamic crack growth in elastomers: experimental energetic analysis

Thomas Corre, Michel Coret, Erwan Verron, Bruno Leblé

Dynamic crack growth in elastomers: experimental energetic analysis

T. Corre
Institut de Recherche en Génie Civil et Mécanique, UMR CNRS 6183, École Centrale de Nantes, France
Naval Group Research, Technocampus Océan, rue de l'Halbranne, 44340 Bouguenais, France.

M. Coret, E. Verron
Institut de Recherche en Génie Civil et Mécanique, UMR CNRS 6183, École Centrale de Nantes, France

B. Leblé
Naval Group Research, Technocampus Océan, rue de l'Halbranne, Bouguenais, France.

ABSTRACT: An experimental procedure allowing full-field measurements during dynamic crack propagation in membranes under large strain is presented. It consists in a two-camera set-up in order to perform digital image correlation during both quasi-static loading and dynamic fracture of the sample. Tested with a highly stretchable polyurethane, this technique permits to retrieve the material configurations of the sample all along crack growth, which is a crucial step toward a complete mechanical analysis of the problem. The dynamic formulation of the J-integral can be computed and its contributions are analysed: the roles of kinetic energy, stress power and strain energy density in the membrane are compared. The applicability of this approach in the case of high speed crack growth is then discussed.

1 INTRODUCTION

The energetic point of view is often favoured when tackling the issue of quasi-static crack growth in elastomer (Thomas 1994). One of the main goals is then to estimate the energy release rate (G) and compare it to its critical value, the fracture energy Γ, to anticipate the failure of the structure. In the case of dynamic fracture, the speed c of the propagating crack becomes the parameter to be predicted. In the classical approach derived from linear elastic fracture mechanics, it is done by equating the instantaneous energy release rate with its critical value at a given speed $\Gamma(c)$ (Freund 1998). The Γ vs. c curve is assumed to be a material parameter for a given elastomer (Greensmith and Thomas 1955). This curve is commonly measured with particular samples that offer a simple fomula for the energy release rate (Rivlin and Thomas 1953, Lake et al. 2000). However, the *J*-integral (Rice 1968) provides a more general way to compute the energy release rate, even if the use of such analytical formulas in an experimental context is challenging. Recently, *J*-integral computation around quasi-static cracks in rubber sheets have been performed, using digital image correlation (DIC) (Caimmi et al. 2015) or particle tracking methods (Qi et al. 2019). Livne et al. (2010) and Goldman Boué et al. (2015) have also computed the *J*-integral around a moving crack in a brittle elastomer, yet under moderate strain level. In the present study, we wish to evaluate the potential of the *J*-integral to understand the behaviour of high speed crack growth in highly stretched membranes. Our experimental set-up that allows DIC measurements during crack propagation is briefly presented, followed by the necessary post-processing steps required to estimated the energy flux integral. A test showing a crack speed of 33m.s^{-1} is then chosen to present the results and to base the discussion on its relevance.

2 EXPERIMENTAL SET-UP

Material

The experiments are carried out with a polyurethane, which can be considered as a typical elastomer: it exhibits a highly non-linear behaviour with a classical S-shape stress-strain curve and breaks at a stretch ratio over 9 in uniaxial tension. Uniaxial tensile tests at constant true strain rate (10^{-3} s^{-1}) have been performed, as shown on Figure 1. We assume that the strain rate is low enough to represent the quasi-static behaviour of the elastomer. This mechanical response is modelled with an isotropic and incompressible hy-

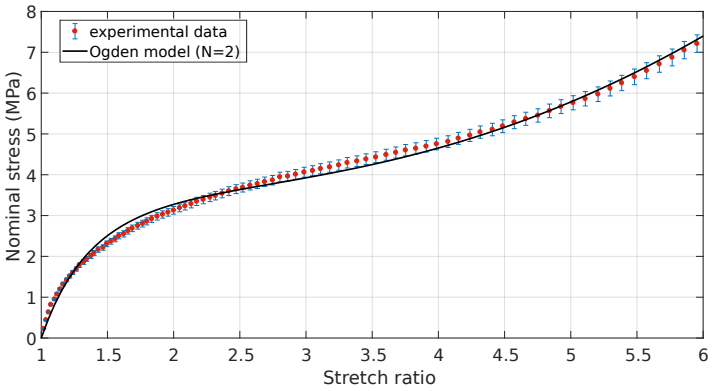

Figure 1: Nominal stress vs stretch ratio in uniaxial tension at a constant strain rate of 10^{-3} s^{-1}. Comparison between experimental data and the 2-term hyperelastic Ogden model.

perelastic constitutive model, the Ogden's model with 4 parameters.

Sample and procedure

"Pure shear" samples are used for the fracture experiments; they are rectangular membranes whose dimensions are $200 \times 40 \times 3$ mm^3. These samples are held in a tensile machine along their longest sides in order to prescribe a vertical stretch ratio denoted λ_y. An experiment consists in two steps:

- the sample is stretched under quasi-static loading conditions until it reaches the prescribed stretch ratio;
- the crack, initiated by a small cut on one of the free edges of the sample at the end of the first step, grows freely through the sample.

The first step (order of magnitude: 5 min) is recorded with a high-resolution camera (29 Mpx) while the second step, much shorter (order of magnitude: 10 ms), is recorded with a high-speed camera whose frame rate ranges between 7000 fps to 25000 fps. Figure 2 shows an example of a picture taken during the crack growth step.

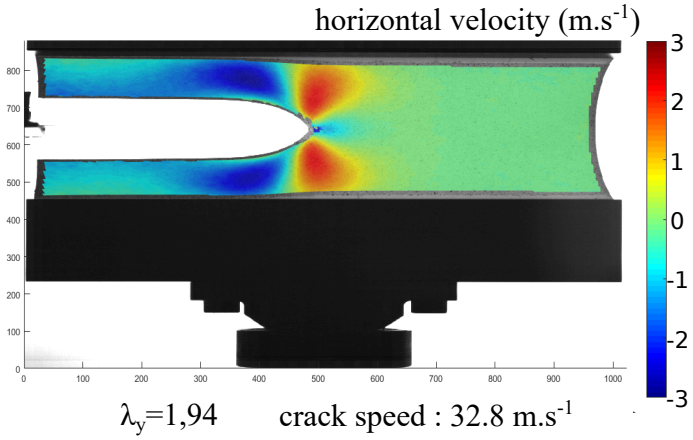

Figure 2: Horizontal velocity field during crack growth. The picture is taken during steady-state crack growth at 32.8 m.s^{-1}.

Full-field measurments

A black speckle is sprayed on the sample to allows digital image correlation during both steps (a commercial software is used). A post-processing step is required to relate the displacement measured by our two distinct cameras: the displacement measured at the end of the first step is projected onto the correlation grid of the high-speed camera at the beginning of step 2. The actual displacement field around the crack tip is the sum of this projected displacement and the one measured from the high-speed film. Moreover, the reference configuration of the sample can be retrieved all along crack growth; it is the cornerstone of a complete mechanical analysis of the fracture process. Then, spatial derivatives of the displacement field are computed using the DIC grid as a finite element mesh. Thanks to the high frame rate we are able to accurately evaluate the time derivatives of the displacement (see Fig. 2 for an example). Finally, the constitutive model is used to calculate the stress field from the strain field, noting that the material parameters have been identified using quasi-static experiments. This method provides a direct measure or an estimate of all the mechanical fields during dynamic crack growth. In particular, the kinetic energy and the strain energy densities fields are available, as shown on Figure 3. Note that the strain energy predominates even in this dynamic context (Fig. 3(c)).

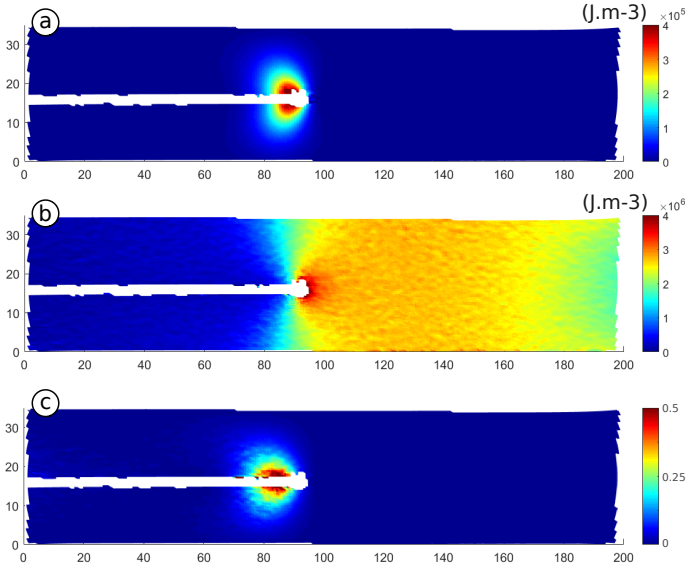

Figure 3: (a) kinetic energy density and (b) strain energy density fields in the reference configuration. (c) ratio between kinetic and strain energy densities. The white line is formed by all the elements where DIC breaks down along the crack path, revealing the crack shape in the reference configuration.

3 ENERGY FLUX MEASUREMENTS

Energy flux definition

The elastodynamic version of the J-integral was proposed by Atkinson and Eshelby (1968) and Freund

(1972), and extended to the non-linear case by Gurtin and Yatomi (1980). It is based on the computation of the flux of mechanical energy entering a contour encircling the crack tip in the reference configuration. Following the presentation by Freund (1998), for a 2D problem with a crack growing along $\vec{e}_1$ at the speed $\vec{c}_0$ in the material configuration, the flux entering the contour Σ of outward normal unit vector $\vec{N}$ is:

$$\Phi(\Sigma) = \int_\Sigma \left[(w+k)\vec{c}_0 + \mathbf{P}^T \cdot \frac{\partial \vec{u}}{\partial t} \right] \cdot \vec{N} \, \mathrm{d}\Sigma, \qquad (1)$$

where w and k are the strain and kinetic energy densities per unit of volume in the reference configuration, ρ_0 is the density of the material in the reference configuration, $\vec{u}$ the displacement field and $\mathbf{P}$ the first Piola-Kirchhoff stress tensor. The corresponding J-integral is then defined by considering a contour that shrinks toward the crack tip:

$$G = \lim_{\Sigma \to 0} \left(\frac{\Phi(\Sigma)}{\|\vec{c}_0\|} \right). \qquad (2)$$

Contrary to the quasi-static case, the integral is not path-independent in general. However, in the case of steady-state crack growth, it is path-independent (Moran and Shih 1987) and the computation of the limit is not necessary.

Practical computation

Crack growth in the pure shear sample exibits a steady-state regime, corresponding to the propagation in the wide area of homogeneous field in the center of the sample. We choose to focus on this particular regime to test the property of path independence of the energy dynamic J-integral. In addition, the horizontal stretch ratio λ_x in the middle of the sample is equal to one. As a consequence, the crack speed in the reference configuration can be easily derived from the speed measured in the deformed configuration (Marder 2006):

$$c_0 = \frac{c}{\lambda_x} = c. \qquad (3)$$

To compute the energy flux integral, we choose circular contours around the crack tip, as illustrated on Figure 4. The circular contours are defined independently from the DIC grid. They are discretised and the value of the vectorial field at each of its nodes is interpolated from the underlying finite element mesh. The scalar product is computed with the outward normal vector and the resulting curve is integrated along the contour. Some elements are missing in the vicinity of the crack tip: high strain level and high material speed cause the DIC to break down at less than 2 mm from the tip. Then, the contour considered have a radius larger than this value.

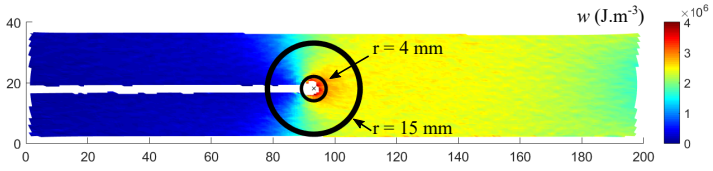

Figure 4: Largest and smallest contours used to compute the energy flux integral. The field is the strain energy density. Imposed stretch ratio: 1.94. Crack speed: 32.8 m.s^{-1}.

4 RESULTS

The energy flux is made of three contributions (Eq. 2) with a quite straightforward interpretation: flux of strain energy, flux of kinetic energy, and the "flux across Σ due to the material outside Σ working on the material inside it"(Moran and Shih 1987). The evolution of these contributions with the radius of the integration contour is presented on Figure 5. With a clear decrease with the radius of the contour, the resulting flux is not path-independent. In spite of the high crack speed, the contribution of the kinetic energy is small compared to the other. It is also negative, as demonstrated theoretically by Gurtin and Yatomi (1980).

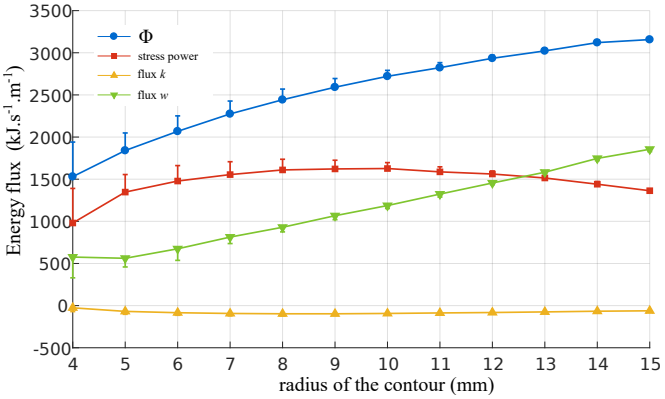

Figure 5: Energy flux and its contribution vs. the contour radius. The error bar indicates the value with an estimate of the contribution close to the crack lips (horizontal extrapolation). These results correspond to the frame on Fig. 4.

To get some insight on the different contributions of the energy flux, the circular contour suggests an angular description of the integrand. The Figure 6 shows the value of each contribution of the integrand along the contour. It is to note that this representation highly depends on the chosen contour. However, the circular path and its radial normal vector seem natural and offer an interpretation of the origin of the energy entering the contour. Then, the strain energy is mainly convected in front of the crack tip while some kinetic energy is convected outside the contour close to the crack lips. The power contribution is important close to the lips (angular position around $\pm 150°$), even if the horizontal speed is low in this area. Indeed, the crack lips experience a high shear strain, making shear components of the Piola-Kirchhoff stress tensor comparable in magnitude to the diagonal ones. In addition, the high vertical velocity still has an important contribution at such angular position. e

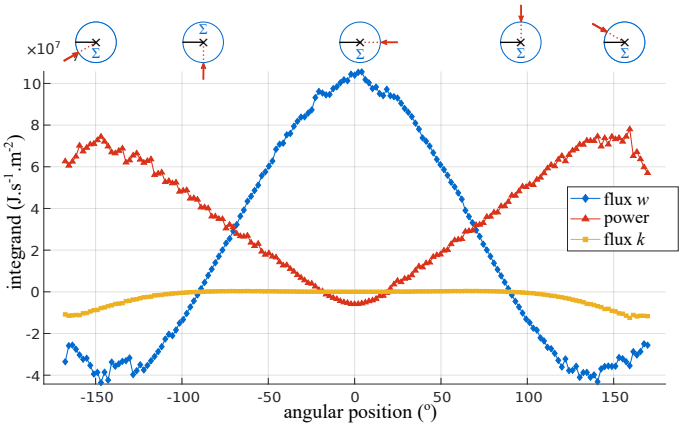

Figure 6: Angular distribution of the energy flux contribution on a contour of radius 7 mm. Small sketches show the positions along the contour with respect to the crack direction.

5 DISCUSSION

This study illustrates that the computation of contour integrals is possible in a dynamic and large strain context with current full-field techniques. The energy flux was computed in a steady-state regime in order to validate the method to estimate the dynamic energy release rate in more complex situations. However, the observed dependence to the contour suggests that something is missing. Having checked the the steady-state crack growth hypothesis and estimated the contribution of the near-lips areas (Fig. 5), two main reasons may explain this result. First, the constitutive model does not take into account the strain rate which is very high, especially behind the crack tip (up to 1500 s^{-1} for the contour on Fig. 6). Therefore, the constitutive equation probably underestimates the stress level in the area behind the crack, reducing the power contribution in the energy flux. Secondly, the material inevitably exhibits a viscoelastic behaviour. Then, some viscous dissipation might occur quite far from the crack tip, especially with highly variable strain rates. Located outside of some contours, it could explain the decrease of the energy flux as the contour radius decreases. These two effects are strongly related to viscoelasticity. Improving the computation of the energy flux would then require a more complex constitutive model that includes a nonlinear viscoelastic contribution. However, being able to identify such a model for strain rates varying from 0 to 1500 s^{-1} remains a challenge.

The increasing role of kinetic energy is sometimes taken as a landmark between a quasi-static and a dynamic fracture problem; marking for instance the only difference between static and dynamic crack tip contour integrals (Freund 1998). However, this analysis reveals the small contribution of the kinetic energy to the energy flux, even if the crack is growing at a speed comparable to the wave speed in the material. This low conversion of elastic energy into kinetic energy is also highlighted by the large difference in the energy density fields. The kinetic energy might not be the most relevant indicator of the dynamics in the case of elastomer membranes and other dynamic effects might come into play before, such as wave reflection (Goldman et al. 2010) or change in the scaling regime for intersonic crack growth (Chen et al. 2011).

REFERENCES

Atkinson, C. & J. Eshelby (1968). The flow of energy into the tip of a moving crack. *International Journal of Fracture Mechanics 4*(1), 3–8.

Caimmi, F., R. Calabr, F. Briatico-Vangosa, C. Marano, & M. Rink (2015). J-integral from full field kinematic data for natural rubber compounds. *Strain 51*(5), 343–356. STRAIN-1068.R1.

Chen, C., H. Zhang, J. Niemczura, K. Ravi-Chandar, & M. Marder (2011). Scaling of crack propagation in rubber sheets. *EPL (Europhysics Letters) 96*(3), 36009.

Freund, L. (1972). Crack propagation in an elastic solid subjected to general loadingi. constant rate of extension. *Journal of the Mechanics and Physics of Solids 20*(3), 129–140.

Freund, L. B. (1998). *Dynamic Fracture Mechanics*. Cambridge University Press.

Goldman, T., A. Livne, & J. Fineberg (2010). Acquisition of inertia by a moving crack. *Physical review letters 104*(11), 114301.

Goldman Boué, T. ., R. Harpaz, J. Fineberg, & E. Bouchbinder (2015). Failing softly: a fracture theory of highly-deformable materials. *Soft Matter 11*, 3812–3821.

Greensmith, H. W. & A. Thomas (1955). Rupture of rubber. iii. determination of tear properties. *Journal of Polymer Science Part A: Polymer Chemistry 18*(88), 189–200.

Gurtin, M. E. & C. Yatomi (1980). On the energy release rate in elastodynamic crack propagation. *Archive for Rational Mechanics and Analysis 74*(3), 231–247.

Lake, G. J., C. C. Lawrence, & A. G. Thomas (2000). High-speed fracture of elastomers: Part I. *Rubber Chemistry and Technology 73*(5), 801–817.

Livne, A., E. Bouchbinder, I. Svetlizky, & J. Fineberg (2010). The near-tip fields of fast cracks. *Science 327*(5971), 1359–1363.

Marder, M. (2006). Supersonic rupture of rubber. *Journal of the Mechanics and Physics of Solids 54*(3), 491–532.

Moran, B. & C. Shih (1987). Crack tip and associated domain integrals from momentum and energy balance. *Engineering Fracture Mechanics 27*(6), 615 – 642.

Qi, Y., Z. Zou, J. Xiao, & R. Long (2019). Mapping the nonlinear crack tip deformation field in soft elastomer with a particle tracking method. *Journal of the Mechanics and Physics of Solids 125*, 326–346.

Rice, J. R. (1968). A path independent integral and the approximate analysis of strain concentration by notches and cracks. *Journal of Applied Mechanics 35*, 379–386.

Rivlin, R. & A. G. Thomas (1953). Rupture of rubber. I. characteristic energy for tearing. *Journal of Polymer Science 10*(10), 291.

Thomas, A. G. (1994). The development of fracture mechanics for elastomers. *Rubber Chemistry and Technology 67*(3), 50–67.